Photo-generated metasurfaces for resonant and high modulation of terahertz signals

Rafik Smaali, Thierry Taliercio, E Centeno

Photo-generated metasurfaces for resonant and high modulation of terahertz signals

R. SMAALI[1,2,*], T. TALIERCIO[3,4], AND E. CENTENO[1,2]

[1]Clermont Université, Université Blaise Pascal, Institut Pascal, BP 10448, F-63000 Clermont-Ferrand,
[2]CNRS, UMR 6602, Institut Pascal, F-63177 Aubière
[3]Université Montpellier, IES, UMR 5214, F-34000, Montpellier, France
[4]CNRS, IES, UMR 5214, F-34000, Montpellier, France
[*]Corresponding author: rafik.smaali@univ-bpclermont.fr

Compiled July 25, 2016

We theoretically demonstrate a resonant modulation of THz waves with photo-designed metasurfaces. Our approach bypasses the issue of the short penetration length of the optical pump which prevents to photo-generate thick metamaterials. We propose a three layers semiconductor system of subwavelength thickness that presents a 100% **modulation of the reflection (or absorption) spectra around 1 THz when it is optically actuated. This resonant modulation can be dynamically monitored at high frequency rate by the optical pump on broad range of frequencies of** $\Delta\nu/\nu = 100\%$**. Finally, appropriate 2D photo-printed patterns make the system polarization insensitive and operational for a wide range of incident angles up to** 65°**.**

OCIS codes: *(230.1150 All-optical devices; (040.2235) Far infrared or Terahertz; (160.3918) Metamaterials;(250.5403) Plasmonics.*

http://dx.doi.org/10.1364/ao.XX.XXXXXX

Terahertz electromagnetic waves of frequencies lying from 0.3 to 10 THz attract much interest owing to their potential applications in several domains ranging from medicine[1], telecommunication[2] or security [3]. Recent developments of bright terahertz (THz) sources and efficient sensors accelerate the progress for non-destructive THz sensing systems [4, 5]. However, in between sources and detectors, THz signals have to be dynamically processed. To respond to this demand, THz devices based on metamaterials have been proposed [6–9]. Metamaterials consist on electromagnetic resonators periodically arranged at the subwavelength scale[10]. They provide a versatile way to dynamically control THz waves by tuning their resonances with external stimuli such as electrical, thermal or mechanical actuations[11]. However, the modulation of the electromagnetic response is generally limited to a narrow spectral range due to the weak frequency variations of the resonator's resonances. Photo-generated metamaterials offer an alternative solution for realizing fully reconfigurable devices that operates over a wide range of frequency [12, 13]. In this approach, the refractive index of a semiconductor layer is locally modified by free carriers which are optically photo-generated by a laser [14–16]. The metamaterials are photo-designed and their patterns resizable as desired allow to dynamically address a broadband of frequency. Additionally, ultra-fast modulation of THz signals is achieved since the photocarriers have a relaxation time in the nanosecond range [17–19]. However, the penetration depth inside the semiconductor for the optical pump is limited to few hundreds of nanometers (at the typical wavelength of a titanium-sapphire laser, 815 nm).[20] This constraint imposes to realize devices of thickness three orders of magnitude smaller than the operating THz wavelength and leads to a weak modulation of the electromagnetic response. Realize ultra-thin metamaterials, also named metasurfaces, which have a high electromagnetic modulation and sharp spectral responses is hence a crucial issue to bring this approach into the application domain. In this Letter, we present an ultra-thin photo-generated absorber whose reflectance and absorbance are modulated with a contrast of 100% at a resonant frequency of 1 THz. This resonance is also demonstrated to be shifted on a wide frequency range of $\Delta\nu = 1$ THz with a modulation contrast higher than 80% when the structural parameters of the metasurface are dynamically varied. Finally, the photo-generated metasurfaces are proven to operate for a wide angular range up to 65° and for any polarization of light.

The metasurface consists of a three layers system InAs / AlSb / n-InAs, Fig. 1a. The top InAs layer is the active material in which a grating pattern is photo-generated. The pump is a Titanium- sapphire laser of wavelength $\lambda_p = 815\,nm$. At this wavelength, the top InAs layer absorbs the pump light (its relative permittivity is 13.64+3.3i) with a penetration distance $l_p = 290\,nm$.[20] This short penetration distance forces to photo-design thin patterns where the concentration of photocarriers is assumed to be uniform. Here, we consider an ultra-thin InAs / AlSb / n-InAs multilayer whose thicknesses are respectively $h = 200\,nm$, $g = 6\,\mu m$ and $s = 500\,nm$, Fig. 1a. Remark that only the refractive index of the top InAs layer is modulated by the pump since its electronic gap (of 0.354 eV) is smaller than that of AlSb (1.616 eV). At THz frequencies, AlSb is a dielectric of relative permittivity $\epsilon_{AlSb} = 12.05$ and plays

the role of a spacer between the top and the n-InAs layers.[20] This last layer is a n-type Si doped InAs semiconductor and acts as a back reflector that forbids the transmission of THz waves through the multilayer. At THz frequency, the relative permittivity of the top InAs is a function of the carrier concentration monitored by the pump intensity. This relative permittivity is determined in the frame work of a Drude model:

$$\epsilon = \epsilon_\infty \left(1 - \frac{\omega_p^2}{\omega^2 + i\omega/\tau}\right) \quad \textbf{(1)}$$

with the plasma frequency $\omega_p = \sqrt{Ne^2/(m_{eff}\epsilon_0\epsilon_\infty)}$ and the decay rate $\tau = \mu m_{eff}/e$. These parameters depend on the carrier concentration N since the mobility μ and the effective mass m_{eff} are modified by the carrier density.[21] We extract N, ω_p and τ from Hall Effect and reflectance measurements. These experimental values are used to adjust the parameters of the following empirical relations: These parameters are fitted from our experimental data and are given by the following empirical relations:[22, 23]

$$\mu = \frac{2}{1 + \sqrt{0.25N10^{-17}}} \ (m^2V^{-1}s^{-1}) \quad \textbf{(2)}$$

$$m_{eff} = (0.02 + 2.3(N)^{0.335} \times 10^{-8})m_0 \quad \textbf{(3)}$$

where m_0 is the electron's mass. When the pump is turned off, the intrinsic concentration in the top InAs layer is $N_i = 7.8 \times 10^{14}\,cm^{-3}$ which corresponds to a dielectric material of relative permittivity $\epsilon_{off} = 8.42 + 1.30i$ at 1 THz, Fig. 1c. When the pump is activated, the top InAs layer switches in a metallic behavior because of the higher photocarrier concentration. For a photocarrier concentration $N = 10^{19}\,cm^{-3}$ which is one order of magnitude smaller compare to recent data obtain for Ge[24], the InAs relative permittivity becomes $\epsilon_{on} = -4745 + 5448i$ at 1 THz, Fig.1d. The back reflector is characterized by a complex permittivity which corresponds to a electronic concentration of $10^{18}\,cm^{-3}$. We utilize this phase transition in order to photo-print 1D or 2D gratings by enlightening selective areas on the top InAs layer, Fig. 1b. Periodic patterns can be photo-induced into the semiconductor with a spatial light modulator[12] or holographic projection for the pump [25]. These approaches allow dynamic variations of the pattern's profile and consequently a real time modulation of the THz signal at typically KHz rate. We start with a 1D grating of pitch $d = 16\,\mu m$ composed of metallic strips (pumped InAs) spaced by dielectric slits (unpumped InAs) of width $f = 0.5\,\mu m$, Fig. 1b. Both reflection R and absorption A spectra are computed for THz p-polarized plane waves (magnetic field parallel to the slits) in normal incidence. These electromagnetic simulations were achieved by using a Rigorous Coupled-Wave Analysis (RCWA) which allows fast and accurate computations of the transmission and reflection coefficients[27]. We define the absorption modulation as the difference of the absorption spectra under and without photo-pumping: $M_A = \mid A_{on} - A_{off} \mid$. By using the same definition, the reflection modulation is noted $M_R = \mid R_{on} - R_{off} \mid$.

Without pumping, the metasurface perfectly reflects the THz plane waves since the n-InAs layer works as a back mirror, Fig. 2a. In that condition, the absorption of the multilayer is negligible: $A_{off} = 0$. The reflection and absorption coefficients are thus related by $R + A = 1$ leading to the same modulation for the reflection and the absorption spectra: $M_A = M_R$. We found that under pumping condition, the metamaterial transforms in a perfect absorber at $\nu = 1$ THz leading to a resonant

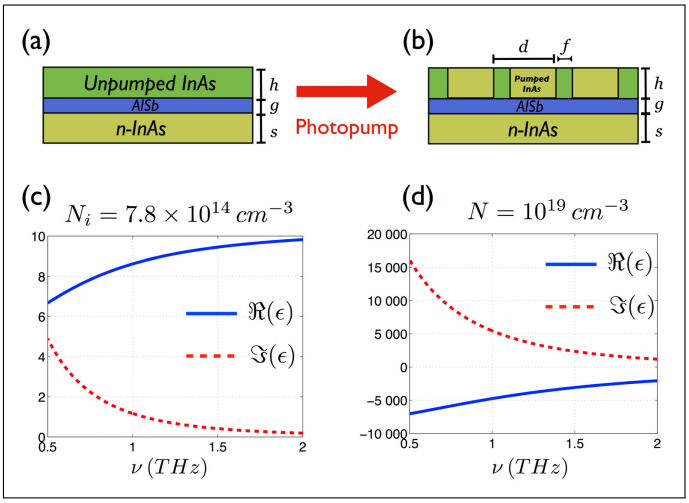

Fig. 1. (Color online) (a) Schematic of the three layer system consisting of a InAs layer, AlSb spacer and a n-InAs back reflector. (b) 1D metasurface photo-designed into the InAs layer. (c) and (d) represent the relative permittivity of InAs for two carrier densities. The real and imaginary parts of the permittivity are respectively plotted in solid and dashed lines.

modulation of the reflection with $M_R = 100\%$, Fig. 2b. This property is explained in terms of a magnetic Fabry-Perot resonance confined at a distance of less than two hundredths of the THz wavelength inside the AlSb spacer. This strong confinement originates from the grating of sub-wavelength slits that emulated an artificial dielectric layer of high refractive index and absorption coefficient. [26]

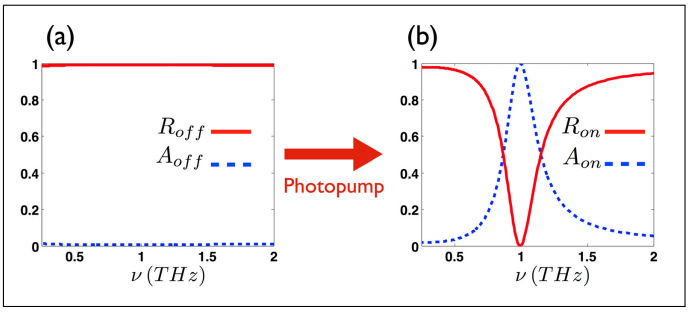

Fig. 2. (a) and (b) are the reflection (solid curve) and absorption (dashed curve) spectra calculated respectively without and with the photopump.

In addition, this absorption line can be shifted over a wide frequency range by modifying the photo-generated grating pitch, Fig. 3a. For a fixed slit's width of $0.5\,\mu m$, the reflection modulation M_R (and absorption modulation M_A) is larger than 80% for a range of frequencies of $\Delta\nu = 1$ THz when the pitch d varies from $7\,\mu m$ to $34\,\mu m$. Equivalently, the variation of the slit's width in the range of $f = [0.13, 4.1]\,\mu m$ for a fixed pitch $d = 16\,\mu m$ leads to a similar frequency behavior for M_R up to 80%, Fig. 3b. Remark that this range of frequencies spans from 0.5 to 2 THz for a modulation of the electromagnetic response higher than 60% which is enough for many applications such as compressive imaging. [28] We underline that the optical patterning for the grating may be realized with a simple interferential system since the width of the slit is larger than the

diffraction limit at the pump wavelength. The metasurface's properties are in addition robust against the variation of the thicknesses for the top layer and the spacer that could be introduced during the fabrication process. Our electromagnetic simulations show that: (i) a relative variation of 50% of the thickness h for the top layer leads to a small shift for the resonance less than 4% with an efficiency larger than 90% and (ii) a relative variation of 17% for the spacer results in a shift of the resonant frequency of 8% with an almost perfect modulation contrast, Fig. 4.

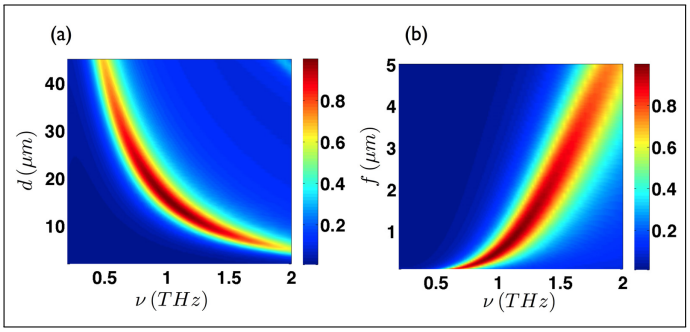

Fig. 3. (a) Reflection modulation M_R (or absorption modulation M_A) as a function of the grating period d and of the THz frequency. The width of the slit is fixed at $f = 0.5\,\mu m$. (b) M_R (or M_A) as a function of the width of the slit f and of the frequency for $d = 16\,\mu m$.

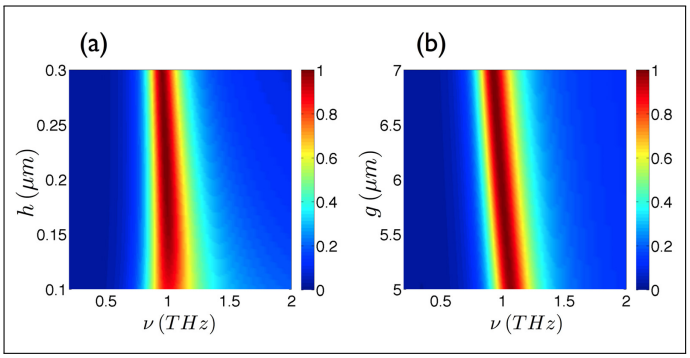

Fig. 4. (a) Reflection modulation M_R (or absorption modulation M_A) as a function of the thickness h for the top InAs layer and of the THz frequency for $g = 6\,\mu m$. (b) M_R (or M_A) as a function of thickness g of the spacer and of the frequency for $h = 200\,nm$.

To extend these properties for any polarization states of light, we consider the same three layer system InAs / AlSb / n-InAs but now the photopump projects a 2D metasurface which consists of a square lattice of subwavelength slits of width $f = 0.5\,\mu m$ periodically spaced with a pitch $d = 16\,\mu m$, Fig. 5(a-b). Here, similar parameters are used for the thicknesses $h = 200\,nm$ and for the back mirror ($500\,nm$) but since the resonance for the 2D metasurface is slightly shifted, the spacer is chosen to $g = 6.8\,\mu m$. This set of parameters is suitable for realizing a perfect absorption at the resonant frequency 1 THz and leads to a 100% reflection modulation when the photopump is activated. Figure 4(d) shows the reflection modulation for a varied angle of incidence θ and for a fixed polarization defined by a magnetic field along one direction of the slits (for a null polarization angle δ). The reflection modulation reveals to be higher than 80% until a grazing incidence of 65°. This property originates from the funneling effect supported by subwavelength slits which work like optical antennas.[29] This large angular efficiency is crucial when a finite size structure enlightened by a Gaussian beam is considered. Indeed, a Gaussian beam can be decomposed in a set of plane waves presenting a varied incident angle. Since the spectral width Δk of the beam is related to its waist W by $W \cdot \Delta k = 2$. We deduce that at 1 THz and for a maximal angle of $\theta_{max} = 65°$, the minimal waist for an efficient modulation is $W = \lambda / (\pi sin\theta_{max})$. This gives $W = 105\mu m$ and shows that a structure of finite size that corresponds to only a third of the THz wavelength would present a modulation of its reflection and absorption higher than 80%. Even more interesting, under normal incidence (for $\theta = 0°$), the 2D photo-generated metasurface perfectly absorbs THz waves for any polarization, Fig. 5(e). The reflection modulation reaches 100% when the polarization angle δ is varied from 0° to 90° which amounts in rotating the magnetic field from one slit direction to the perpendicular one. We remark that the wide angular aperture is also interesting when a finite size structure

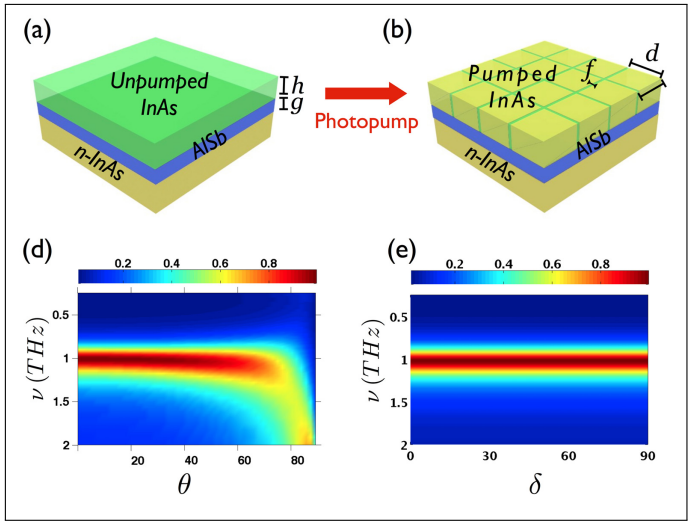

Fig. 5. (a) Schematic of the three layer system. (b) Metasurface photo-designed into the InAs layer. (d) Modulation parameter M_R as a function of the frequency and of the incident angle θ for a fixed polarization angle $\delta = 0°$. (e) M_R as a function of the frequency and of the polarization angle δ in normal incidence ($\theta = 0°$).

In conclusion, we have demonstrated a resonant 100% switch of the electromagnetic response for photo-designed metasurfaces at THz frequencies. This resonant response centered at 1 THz is proven to shift over a large frequency range of 1 THz when the structural parameters of the metasurfaces (grating's pitch, slit's width) are varied. Finally, these properties become insensitive to the polarization of light and to the incident angle until 65° when 2D metasurfaces are photo-generated. Compare to electrically actuated graphene based modulators, which present a high modulation rate between 40 to 100 MHz [30, 31], our optically generated metasurface has a lower modulation rate about 1 KHz. However, the latter approach is more versatile since the dynamically modification of the metasurface offers an efficient solution for operating on a broad range of frequency.

REFERENCES

1. E. Pickwell and V. P. Wallace, J. Phys. D Appl. Phys., **39**, R301 (2006).
2. S. Koenig, D. Lopez-Diaz, J. Antes, and F. Boes, Nat. Photonics **7**, 977 (2013).
3. J. F. Federici, B. Schulkin, F. Huang, D. Gary, R. Barat, F. Oliveira, and D. Zimdars, Semicond. Sci. Technol., **20**, S266 (2005).
4. G. Liang, X. Hu, X. Yu, Y. Shen, L. H. Li, A. G. Davies, E. H. Linfield, H. K. Liang, Y. Zhang, S. F. Yu, and Q. J. Wang, ACS Photonics, **2**, 1559 (2015).
5. M. Tonouchi, Nat. Photonics **1**, 97 (2007).
6. K. Fan, A. C. Strikwerda, X. Zhang, and R. D. Averitt, Phys. Rev. B **87**, 161104 (2013).
7. J. Gu, R. Singh, X. Liu, X. Zhang, Y. Ma, S. Zhang, S. A. Maier, Z. Tian, A. K. Azad, H.-T. Chen, A. J. Taylor, J. Han, and W. Zhang, Nat. Communications **3**, 1151 (2012).
8. J. Zhou, Y.-S. Park, J. Rho, R. Singh, S. Nam, A. K. Azad, H.-T. Chen, X. Yin, S. Zhang, A. J. Taylor, and X. Zhang, Nat. Communications **3**, 942 (2012).
9. L. Ren, C. L. Pint, T. Arikawa, K. Takeya, I. Kawayama, M. Tonouchi, R. H. Hauge, and J. Kono, Nano Lett. **12**, 787 (2012).
10. D. Smith, J. Pendry, and M. Wiltshire, Science **305**, 788 (2004).
11. K. Fan and W. J. Padilla, Materials Today **18**, 39 (2015).
12. T. Okada and K. Tanaka, Scientific Reports **1**, 121 (2011).
13. I. Chatzakis, P. Tassin, L. Luo, N.-H. Shen, L. Zhang, J. Wang, T. Koschny, and C. M. Soukoulis, Appl. Phys. Lett., **103**, 043101 (2013).
14. F. P. Mezzapesa, L. L. Columbo, C. Rizza, M. Brambilla, A. Ciattoni, M. Dabbicco, M. S. Vitiello, and G. Scamarcio, Scientific Reports **5**, 16207 (2015).
15. S. J. Allen Jr, D. C. Tsui, and R. A. Logan, Phys. Rev. Lett. **38**, 980 (1977).
16. H. J. Eichler, F. Massmann, E. Biselli, K. Richter, and M. Glotz, Phys. Rev. B **36**, 3247 (1987).
17. M. C. Schaafsma and J. G. Rivas, Semicond. Sci. Technol. **28**, 124003 (2013).
18. T. P. Steinbusch, H. K. Tyagi, M. C. Schaafsma, G. Georgiou, and J. G. Rivas, Opt. Express **22**, 26559 (2014).
19. G. Georgiou, H. K. Tyagi, P. Mulder, G. J. Bauhuis, J. J. Schermer, and J. G. Rivas, Scientific Reports, **4**, 3584 (2014).
20. E. D. Palik, *Handbook of Optical Constants of Solids II* (Academic Press 1991).
21. C. Rizza, A. Ciattoni, E. Spinozzi, and L. Columbo, Opt. Lett., **37**, 3345 (2012).
22. C. Hilsum, Electron. Lett. **10**, 259 (1974).
23. M. P. Mikhailova, *in Handbook series on semiconductor parameters* M. Levinshtein, S. Rumyantsev and M. Shur, ed., (World Scientific, 1996) vol. I, pp. 14768.
24. B. Mayer, C. Schmidt, J. Bhler, D. V. Seletskiy, D. Brida, A. Pashkin, and A. Leitenstorfer, New Journal of Physics, **16**, 063033 (2014).
25. Y. Hayasaki, T. Sugimoto, A. Takita, and N. Nishida, Appl. Phys. Lett., **87**, 031101 (2005).
26. J. T. Shen, P. B. Catrysse, and S. Fan, Phys. Rev. Lett. **94**, 197401 (2005).
27. T. Weiss, G. Granet, N.A.Gippius, S.G. Tikhodeev, Opt. Expr. **17**, 8051 (2009).
28. C.M. Watts, D. Shrekenhamer, J. Montoya, G. Lipworth, J. Hunt, T. Sleasman, S. Krishna, D.R. Smith, and W.J. Padilla, Nat. Photonics, **8**, 605 (2014).
29. F. Pardo, P. Bouchon, R. Hadar, and J.-L. Pelouard, Phys. Rev. Lett. **107**, 093902 (2011).
30. S. A. Mikhailov, N. A. Savostianova, F. Valmorra, J. E. R. O. M. Faist, G. R. Nash, P. Q. Liu, and I. J. Luxmoore, Nat. Comm. **6**, 1 (2015).
31. D. S. Jessop, S. J. Kindness, L. Xiao, P. Braeuninger-Weimer, H. Lin, Y. Ren, C. X. Ren, S. Hofmann, J. A. Zeitler, H. E. Beere, D. A. Ritchie, and R. Degl´ Innocenti, Appl. Phys. Lett. **108**, 171101 (2016).

REFERENCES

1. E. Pickwell and V. P. Wallace, "Biomedical applications of terahertz technology", J. Phys. D Appl. Phys., **39**, R301 (2006).
2. S. Koenig, D. Lopez-Diaz, J. Antes, and F. Boes, "Wireless sub-THz communication system with high data rate", Nat. Photonics **7**, 977 (2013).
3. J. F. Federici, B. Schulkin, F. Huang, D. Gary, R. Barat, F. Oliveira, and D. Zimdars, "THz imaging and sensing for security applications-explosives, weapons and drugs", Semicond. Sci. Technol., **20**, S266 (2005).
4. G. Liang, X. Hu, X. Yu, Y. Shen, L. H. Li, A. G. Davies, E. H. Linfield, H. K. Liang, Y. Zhang, S. F. Yu, and Q. J. Wang, "Integrated terahertz graphene modulator with 100% modulation depth", ACS Photonics, **2**, 1559 (2015).
5. M. Tonouchi, "Cutting-edge terahertz technology", Nat. Photonics **1**, 97 (2007).
6. K. Fan, A. C. Strikwerda, X. Zhang, and R. D. Averitt, "Three-dimensional broadband tunable terahertz metamaterials", Phys. Rev. B **87**, 161104 (2013).
7. J. Gu, R. Singh, X. Liu, X. Zhang, Y. Ma, S. Zhang, S. A. Maier, Z. Tian, A. K. Azad, H.-T. Chen, A. J. Taylor, J. Han, and W. Zhang, "Active control of electromagnetically induced transparency in a terahertz metamaterial", Nat. Communications **3**, 1151 (2012).
8. J. Zhou, Y.-S. Park, J. Rho, R. Singh, S. Nam, A. K. Azad, H.-T. Chen, X. Yin, S. Zhang, A. J. Taylor, and X. Zhang, "Photoinduced handedness switching in terahertz chiral metamolecules", Nat. Communications **3**, 942 (2012).
9. L. Ren, C. L. Pint, T. Arikawa, K. Takeya, I. Kawayama, M. Tonouchi, R. H. Hauge, and J. Kono, "Broadband terahertz polarizers with ideal performance based on aligned carbon nanotube stacks", Nano Lett. **12**, 787 (2012).
10. D. Smith, J. Pendry, and M. Wiltshire, "Metamaterials and negative refractive index", Science **305**, 788 (2004).
11. K. Fan and W. J. Padilla, "Dynamic electromagnetic metamaterials", Materials Today **18**, 39 (2015).
12. T. Okada and K. Tanaka, "Photo-designed terahertz devices", Scientific Reports **1**, 121 (2011).
13. I. Chatzakis, P. Tassin, L. Luo, N.-H. Shen, L. Zhang, J. Wang, T. Koschny, and C. M. Soukoulis, "One-and two-dimensional photo-imprinted diffraction gratings for manipulating terahertz waves", Appl. Phys. Lett., **103**, 043101 (2013).
14. F. P. Mezzapesa, L. L. Columbo, C. Rizza, M. Brambilla, A. Ciattoni, M. Dabbicco, M. S. Vitiello, and G. Scamarcio, "Photo-generated metamaterials induce modulation of CW terahertz quantum cascade lasers", Scientific Reports **5**, 16207 (2015).
15. S. J. Allen Jr, D. C. Tsui, and R. A. Logan, "Observation of the Two-Dimensional Plasmon in Silicon Inversion Layers", Phys. Rev. Lett. **38**, 980 (1977).
16. H. J. Eichler, F. Massmann, E. Biselli, K. Richter, and M. Glotz, "Laser-induced free-carrier and temperature gratings in silicon", Phys. Rev. B **36**, 3247 (1987).
17. M. C. Schaafsma and J. G. Rivas, " Semiconductor plasmonic crystals : active control of THz extinction", Semicond. Sci. Technol. **28**, 124003 (2013).
18. T. P. Steinbusch, H. K. Tyagi, M. C. Schaafsma, G. Georgiou, and J. G. Rivas, "Active terahertz beam steering by photo-generated graded index gratings in thin semiconductor films", Opt. Express **22**, 26559 (2014).
19. G. Georgiou, H. K. Tyagi, P. Mulder, G. J. Bauhuis, J. J. Schermer, and J. G. Rivas, "Photo-generated THz antennas", Scientific Reports, **4**, 3584 (2014).
20. E. D. Palik, "*Handbook of Optical Constants of Solids II*", (Academic Press 1991).
21. C. Rizza, A. Ciattoni, E. Spinozzi, and L. Columbo, "Terahertz active spatial filtering through optically tunable hyperbolic metamaterials", Opt. Lett., **37**, 3345 (2012).
22. C. Hilsum, "Simple empirical relationship between mobility and carrier concentration", Electron. Lett. **10**, 259 (1974).
23. M. P. Mikhailova, "*in Handbook series on semiconductor parameters*", M. Levinshtein, S. Rumyantsev and M. Shur, ed., (World Scientific, 1996) vol. I, pp. 14768.
24. B. Mayer, C. Schmidt, J. Bhler, D. V. Seletskiy, D. Brida, A. Pashkin, and A. Leitenstorfer, "Sub-cycle slicing of phase-locked and intense mid-infrared transients", New Journal of Physics, **16**, 063033 (2014).
25. Y. Hayasaki, T. Sugimoto, A. Takita, and N. Nishida, "Variable holographic femtosecond laser processing by use of a spatial light modulator", Appl. Phys. Lett., **87**, 031101 (2005).
26. J. T. Shen, P. B. Catrysse, and S. Fan, "Mechanism for Designing Metallic Metamaterials with a High Index of Refraction", Phys. Rev. Lett. **94**, 197401 (2005).
27. T. Weiss, G. Granet, N.A.Gippius, S.G. Tikhodeev, "Matched coordinates and adaptive spatial resolution in the Fourier modal method", Opt. Expr. **17**, 8051 (2009).
28. C.M. Watts, D. Shrekenhamer, J. Montoya, G. Lipworth, J. Hunt, T. Sleasman, S. Krishna, D.R. Smith, and W.J. Padilla,"Terahertz compressive imaging with metamaterial spatial light modulators", Nat. Photonics, **8**, 605 (2014).
29. F. Pardo, P. Bouchon, R. Hadar, and J.-L. Pelouard, "Light Funneling Mechanism Explained by Magnetoelectric Interference", Phys. Rev. Lett. **107**, 093902 (2011).
30. S. A. Mikhailov, N. A. Savostianova, F. Valmorra, J. E. R. O. M. Faist, G. R. Nash, P. Q. Liu, and I. J. Luxmoore,"Highly tunable hybrid metamaterials employing split-ring resonators strongly coupled to graphene surface plasmons", Nat. Comm. **6**, 1 (2015).
31. D. S. Jessop, S. J. Kindness, L. Xiao, P. Braeuninger-Weimer, H. Lin, Y. Ren, C. X. Ren, S. Hofmann, J. A. Zeitler, H. E. Beere, D. A. Ritchie, and R. Degl´ Innocenti, "Graphene based plasmonic terahertz amplitude modulator operating above 100 MHz", Appl. Phys. Lett. **108**, 171101 (2016).